

Experimental study on seepage characteristics of large size rock specimens under three-dimensional stress

Wenbin Sun^{*1}, Yanchao Xue^{1,2a}, Liming Yin^{1b} and Junming Zhang¹

¹College of Mining and Safety Engineering, Shandong University of Science and Technology, Qingdao 266590, People's Republic of China

²School of Resources & Civil Engineering, Northeastern University, Shenyang 110819, People's Republic of China

(Received March 22, 2019, Revised July 29, 2019, Accepted July 31, 2019)

Abstract. In order to study the effect of stress and water pressure on the permeability of fractured rock mass under three-dimensional stress conditions, a single fracture triaxial stress-seepage coupling model was established; By using the stress-seepage coupling true triaxial test system, large-scale rock specimens were taken as the research object to carry out the coupling test of stress and seepage, the fitting formula of permeability coefficient was obtained. The influence of three-dimensional stress and water pressure on the permeability coefficient of fractured rock mass was discussed. The results show that the three-dimensional stress and water pressure have a significant effect on the fracture permeability coefficient, showing a negative exponential relationship. Under certain water pressure conditions, the permeability coefficient decreases with the increase of the three-dimensional stress, and the normal principal stress plays a dominant role in the permeability. Under certain stress conditions, the permeability coefficient increases when the water pressure increases. Further analysis shows that when the gob floor rock mass is changed from high stress to unloading state, the seepage characteristics of the cracked channels will be evidently strengthened.

Keywords: single fractured rock mass; stress-seepage coupling; true triaxial test system; floor water-inrush

1. Introduction

The seepage problem in rock mass, especially the seepage problem under the influence of ground stress, water pressure and mining disturbance, is a key and difficult problem facing many engineering disciplines (Li et al. 2017, Javadi et al. 2010, Khanh et al. 2018, Miao et al. 2015, Al-Shukur et al. 2018, Sun and Xue 2018, Kong et al. 2019). The floor water inrush accident in mining engineering is a typical fluid solid coupling problem under high stress (Odintsev and Miletenko 2015, Sun et al. 2019, Shao et al. 2019). The permeability characteristics of water inrush channel in floor can be regarded as confined water permeability characteristics of the floor rock mass propagating along joints and fissures under three-dimensional stress, Water pressure and stress conditions are the main factors affecting the seepage characteristics of rock mass. (Yang et al. 2014, Konsoer et al. 2015, James et al. 2018). If macroscopic considering a single water inrush channel, the seepage characteristics of single fracture surface should be studied (Nguyen-Thoi et al. 2015, Lv et al. 2019).

As a basic topic of seepage research in fractured rock mass, single fracture stress-seepage coupling has been studied through a lot of theoretical, numerical simulation and experimental researches from many aspects by many research scholars at home and abroad (Di et al. 2017, Giwelli et al. 2014, Haeri et al. 2014, Wu et al. 2019). Snow (1968) proposed an empirical model for describing the variation of permeability with positive strain; Louis (1987) described the linear relationship between the permeability coefficient of smooth and parallel fractures and the square of the fracture aperture, and put forward the generally accepted square law of the smooth fracture model; Tsang and Tsang (2004) proposed cubic law for grooved flow model; However, none of these fractured hydraulic models can reflect the influence of rock three-dimensional stress field on permeability. Morrow et al. (2014) and Yasuhara et al. (2006) studied the influence of the change of effective stress on the permeability of single fractured rock mass during cyclic loading; Pantelis (2006) and Liu (2013) studied the seepage problem of multi-fissured rock mass. Chang et al. (2004) experimental studied the coupling relationship between the fracture permeability and the triaxial stress, and gave the formula of the permeability coefficient of the three-dimensional stress response using 100 mm (width) × 100 mm (height) × 200 mm (length) rock specimen; Tao and Liu (2012) used a 50 mm × 50 mm × 100 mm rock mass specimen to carry out seepage characteristics study by Matlab program, and the relationship between equivalent seepage resistance, permeability and stress in fractured rock mass was obtained; Yu et al. (2012) studied the seepage

*Corresponding author, Ph.D.
E-mail: swb@sdust.edu.cn

^aPh.D. Student
E-mail: stxycgs@126.com

^bPh.D.
E-mail: yinlimin@sdust.edu.cn

characteristics under the loading and unloading of fractured sandstone and siltstone with cylindrical specimens of 45 mm–50 mm in diameter, and numerical simulation was applied to analyze the change rule of the permeability and the seepage velocity; Experimental study of shear displacement effect seepage characteristics of random surface cracks was carried out through experiment on 200 mm × 100 mm × 100 mm rock specimen by Lei *et al.* (2016); Theoretical and experimental investigation of characteristics of single fracture stress-seepage coupling considering microroughness was carried out through experiment on 100 mm × 100 mm × 200 mm rock specimen by Di *et al.* (2017). In addition, many scholars establish the relationship between the permeability coefficient and the stress through seepage tests under different confining pressures and different hydraulic gradients (Miao *et al.* 2015, Bandis *et al.* 1983, Goodman 1976, Develi and Babadagli 2015, Jaksa 2007, Liu and Chen 2007, Sun *et al.* 2019).

Most of the above studies are based on small size rock specimens because it is difficult to study large size rock specimens, which requires higher requirements for equipment. However, with the increase of fracture surface size, the displacement at peak strength increases, and the shear failure mode changes from brittle failure to ductile failure. The larger rock size is beneficial to analyze the seepage evolution of the main fracture system in the stress field of the seepage area in rock mass with a large proportion of fissures, and better reflect the actual situation in the field. In this study, a large number of laboratory tests have been carried out on large rock specimens (200 mm × 200 mm × 400 mm, at least twice the size of previous studies) using the stress-seepage coupling true triaxial test system for high water pressure rock independently developed by our research group. The effects of three-dimensional stress and osmotic pressure on fracture permeability are discussed.

2. Materials and methods

2.1 Fracture seepage and triaxial stress coupling model

It is assumed that the flow condition of water in the fractures is laminar flow; the water is incompressible and viscous in the process; the water flow only seeps along fracture surfaces without other loss of flow; the fissure water pressure acting on fracture surfaces is regarded as the average head pressure at the inlet and outlet ends. Fig. 1 shows the calculation model of single fracture under stress-seepage coupling.

As shown in Fig. 1, owing to the narrow fracture and no filling, the lateral deformation of the single fracture of specimen is equal to the lateral strain of the two bedrock blocks (Cai *et al.* 2002), then

$$\left. \begin{aligned} \varepsilon_1 &= \frac{1}{E_r} [\sigma_1 - \nu_r (\sigma_2 + \sigma_3)] \\ \varepsilon_3 &= \frac{1}{E_r} [\sigma_3 - \nu_r (\sigma_2 + \sigma_1)] \end{aligned} \right\} \quad (1)$$

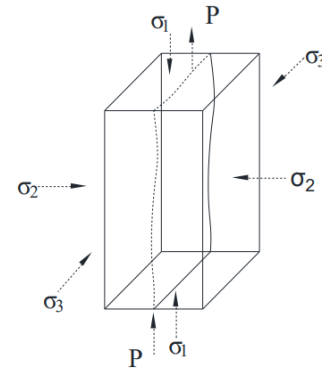


Fig. 1 Calculation model of single fracture under stress-seepage coupling

where $\sigma_1, \sigma_2, \sigma_3$ are the three direction principal stresses, E_r is the elastic modulus of rocks, ν_r is the poisson's ratio, ε_1 and ε_2 are the lateral strain of the two bedrock blocks.

The lateral deformation of the single fracture can be expressed as

$$\begin{aligned} \varepsilon_s &= \varepsilon_1 + \varepsilon_3 = \frac{1}{E_r} [\sigma_1 - \nu_r (\sigma_2 + \sigma_3)] \\ &+ \frac{1}{E_r} [\sigma_3 - \nu_r (\sigma_2 + \sigma_1)] \\ &= \frac{1 - \nu_r}{E_r} (\sigma_1 + \sigma_3) - \frac{2\nu_r}{E_r} \sigma_2 \end{aligned} \quad (2)$$

Then according to Hooke's law, the normal deformation of the single fracture can be expressed as

$$\varepsilon_n = \frac{\sigma_2 - aP}{k_n} - \frac{\nu_f}{k_s} (\sigma_1 + \sigma_3) \quad (3)$$

In formula (3), a is the coefficient of influence considering pore roughness on pore water pressure, p is the hydraulic pressure along the side of the fracture, ν_f is the Poisson's ratio of the fracture, k_n is the normal elastic modulus of the fracture, k_s is the tangential elastic modulus of the fracture.

Supposing the initial width of the fracture is d_0 , therefore, the constitutive equation of fracture deformation u is

$$\varepsilon_n = \frac{\sigma_2 - aP}{k_n} - \frac{\nu_f}{k_s} (\sigma_1 + \sigma_3) \quad (4)$$

After deformation, the width of the fracture is $d = d_0 - u = d_0 e^{-\varepsilon_n}$.

Since the seepage of fractured rock masses is only related to the fracture width or aperture, in order to overcome the difficulty of determining the width of fractures and to consider the effect of fracture roughness on seepage, according to the well-known square law of percolation of smooth fractured rock mass $k = \frac{gd^2}{12\mu}$, with d introduced into $k = \frac{gd_0^2}{12\mu} e^{-2\varepsilon_n}$, then

$$k = k_0 e^{-2\varepsilon_n} \quad (5)$$

where k_0 is the initial permeability coefficient of fractured rock mass.

With Formula (3) introduced into (5)

$$k = k_0 e^{-2 \left[\frac{\sigma_2 - aP}{k_n} \frac{v_f}{k_s} (\sigma_1 + \sigma_3) \right]} \quad (6)$$

Since the roughness of the fracture affects both the normal deformation and the two lateral deformations of the fracture under three-dimensional stress, however, the seepage state of the fracture depends only on the normal deformation of the fracture, the normal deformation of the fracture is related to the three-dimensional stress suffered by the fracture and the osmotic pressure, the normal and tangential elastic modulus of the fracture and the Poisson's ratio caused by the roughness of the fracture. So formula (6) can be simplified

$$k = k_0 e^{-2[b(\sigma_2 - aP) - c(\sigma_1 + \sigma_3)]} \quad (7)$$

where b is the coefficient of influence of the roughness of the fracture on the normal elastic modulus of the fracture, c is the coefficient of influence of the roughness of the fracture on the ratio of Poisson's ratio and tangential elastic modulus of the fracture.

Formula (7) is the theoretical mathematical model of single fracture stress-seepage coupling. According to formula (7), when the rock mass is subjected to large normal stress, the width of fracture decreases sharply, and its seepage rule tends to the law of seepage in quasi continuum rock mass

2.2 Test conditions and methods

2.2.1 Test conditions

The experimental equipment uses the stress-seepage coupling true triaxial test system for high water pressure rock independently developed by our research group, as shown in Fig. 2. The test system is made up of three axis loading frame, three axle loading mechanism, high pressure water seepage system, test box, numerical control system and data acquisition system, and other components, the principle is shown in Fig. 3. Loading test device has constant triaxial stress, constant triaxial displacement and constant triaxial stiffness of three controllable conditions. The test box is open design, replacing the corresponding indenters and components, and applying osmotic pressure on the shear direction of parallel fractures, the fracture shear penetration test of rock, cement, geotechnical and other specimens, and permeability and mechanical properties test of fractured rock mass under triaxial unloading can be carried out

The key technical indicators of the test system are mainly reflected in the true triaxial loading unit and its servo control part, seepage loading unit and its servo regulator system. The three direction load of the test bench is 1,600 kN, 1,000 kN and 500 kN, respectively. The deformation is controlled by the mean value of multi branch displacement sensors, and the measurement accuracy is up to 1% of the indicating value. In the servo control part, the minimum and maximum loading rates are 0.01 kN/s and



Fig. 2 Stress-seepage coupling true triaxial test system for high water pressure rock

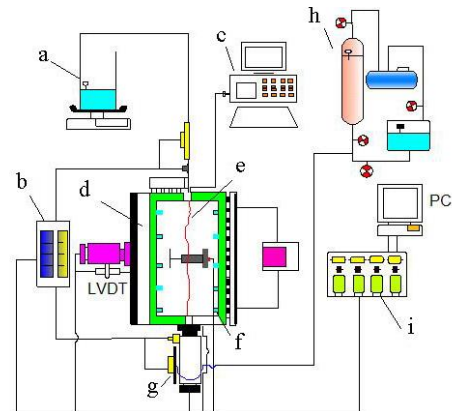


Fig. 3 Schematic diagram of the test system: (a) Water collection; (b) Osmotic pressure measuring and controlling device (c) Acoustic measurement system; (d) Test box device; (e) Joint surface; (f) Acoustic emission probe; (g) Flow meter; (h) Osmotic pressure stabilizing device; (i) Multifunction control panel

Table 1 Physico-mechanical properties of the specimen

Density / $\text{kg}\cdot\text{m}^{-3}$	Compressive strength /MPa	Elastic modulus / 10^3MPa	Poisson's ratio μ	Tensile strength /MPa	Cohesion /MPa	Internal friction angle $\varphi/^\circ$
2506	112.7	52.2	0.22	4.6	18.3	55

100 kN/s, respectively. Loading can be done in two ways, rigid loading or rigid and flexible mixed loading according to the experimental purpose. The maximum sealing water pressure (osmotic pressure) of osmotic pressure servo control system can reach 5 MPa and the osmotic pressure stabilizes for 10 days. The minimum and maximum measuring ranges of water flow are $0.001 \text{ mL}\cdot\text{s}^{-1}$ and $2 \text{ mL}\cdot\text{s}^{-1}$, the accuracy of the related measurement and control is up to 1% of the indicating value.

2.2.2 Test methods

The experiment mainly considered the influence of water pressure and three-dimensional stress on the seepage characteristics of the structural plane, and ignored the effect of lithology. Granite rock samples were used for the test. The physical and mechanical parameters are shown in Table 1. Using large-size rock samples, processed into $200 \text{ mm} \times 200 \text{ mm} \times 400 \text{ mm}$ rectangular parallelepiped specimens,



Fig. 4 Intact rock samples



Fig. 5 Rock sample after splitting



Fig. 6 Sealed capsule



Fig. 7 Test box device

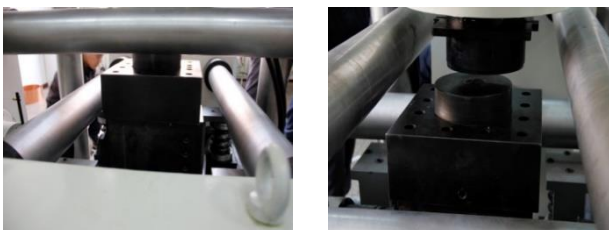


Fig. 8 Test operation

the current study of rock mass seepage characteristics of the literature (Lei *et al.* 2016, Liu and Chen 2007, Zhang and Zhang 1997, Wu 2010) has not been reported; After grinding the sides to the required accuracy of the test, the splitting experimental mode was used to form the experimental fracture of the rock specimen to simulate the tensional fissure state, as shown in Fig. 4 and Fig. 5.

After the sample was saturated with water for 7 days, it was loaded into the pre-made capsule, seal between the capsule and the sample with a sealant, and smear butter evenly on the outer side of the capsule and paste thin copper sheet of the same size as the sample area, then, after smear large butter on the outside of thin copper sheet, put it into a test box, and the test box is evenly locked and sealed and then hoisted into the test machine for test. Fig. 6 is the sealed capsule. Fig. 7 is the test box, and the test process is shown in Fig. 8.

3. Results and discussion

3.1 Sample roughness

When the groundwater flows in the fracture, the roughness of the fracture surface is the key factor affecting the stress-seepage characteristics of the joint. The roughness of the fracture surface is defined as the waviness and undulation of the fracture surface relative to the reference plane. At present, the methods of describing the roughness mainly include convex height characterization method, joint roughness coefficient JRC characterization method and fractal characterization method. The roughness coefficient JRC was used to characterize the roughness of the fractured rock in this test. The laboratory used TR600 contour roughness measuring instrument to measure the test rock samples, and a total of 22 feature sampling lengths were selected. Fig. 9 is the TR600 contour roughness measuring instrument, Fig. 10 is a distribution map of the length of each sample on a fracture surface, Fig. 11 shows the H-11 profile roughness measurement test results.

Tse and Cruden (1979) used empirical relationships to calculate the roughness factor of a typical fracture

$$JRC = 32.2 + 32.47 \lg \left[1 / MD_x^2 \sum_{i=1}^M (y_{i+1} - y_i) \right]^{1/2} \quad (8)$$

where M is the interval number for measuring the height of roughness; D_x represents the sample interval length of the roughness measurement; y_i and y_{i+1} are rough heights of the i th and $(i+1)$ th points.

The statistical JRC values of #1 and #2 specimens are 12.7 and 15.1, respectively, with the results of (8) and the measurement results of contour roughness measuring instrument.

3.2 Test results

The test box was put in the test machine and made a good location, and the axial pressure σ_1 , lateral pressure σ_2 and σ_3 and osmotic pressure were added to the set initial value. Change the axial pressure, the lateral pressure and

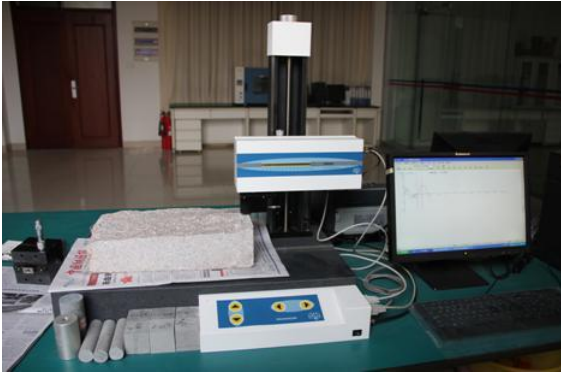


Fig. 9 TR600 measuring instrument of contour roughness

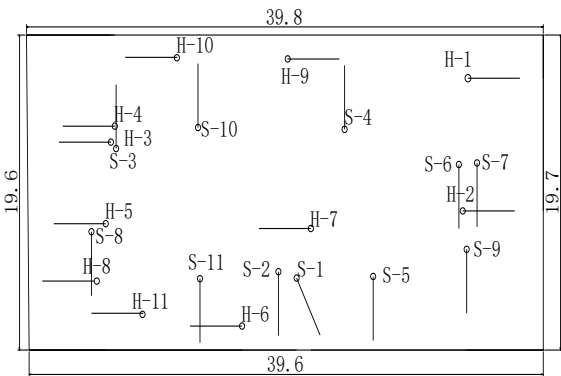


Fig. 10 Distribution diagram of sample length in fracture surface

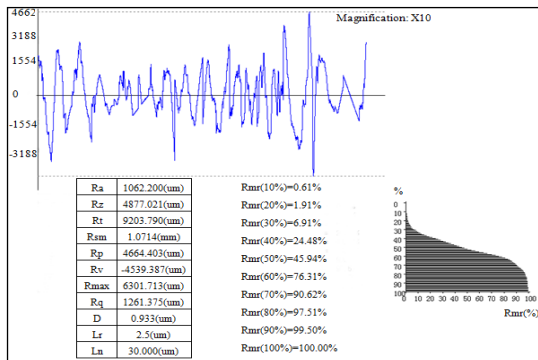


Fig. 11 H-11 testing results of contour roughness

the seepage water pressure to measure the water yield within certain period of time.

Testes of specimens #1 and #2 were carried out under different combinations of three-dimensional principal stress and osmotic pressure. The test results are shown in Tables 2 and 3.

3.3 Results analysis

The roughness of the fracture affects both the normal deformation and the two lateral deformations of the fracture under three-dimensional stress, the seepage state of the fracture depends only on the normal deformation of the fracture; The normal deformation of the fracture is related to three-dimensional stress subjected to the fracture and seepage water pressure, tangential and normal elastic

Table 2 Test data sheet of permeability coefficient of #1 granite specimen ($10^{-5} \text{ cm} \cdot \text{s}^{-1}$)

σ_1 /MPa	σ_2 /MPa	σ_3 /MPa	Osmotic pressure P /MPa				
			1	2	3	4	5
5	3	3	1.029	1.159			
	4	3	0.884	0.994			
	5	3	0.751	0.824			
10	5	4	0.686	0.614	0.864		
	5	4	0.726	0.828	0.987		
	5	5	0.728	0.784	0.865	1.027	
15	6	5	0.599	0.574	0.758	0.852	
	7	5	0.576	0.532	0.628	0.729	
	8	5	0.416	0.467	0.524	0.586	
20	9	5	0.353	0.384	0.382	0.486	
	10	5	0.283	0.318	0.328	0.403	
	10	6	0.281	0.331	0.372	0.385	0.450
30	11	6	0.233	0.232	0.295	0.331	0.373
	12	6	0.193	0.217	0.245	0.275	0.309
30	12	6	0.186	0.175	0.197	0.205	0.249

Table 3 Test data sheet of permeability coefficient of #2 granite specimen ($10^{-5} \text{ cm} \cdot \text{s}^{-1}$)

σ_1 /MPa	σ_2 /MPa	σ_3 /MPa	Osmotic pressure P /MPa				
			1	2	3	4	5
5	3	3	2.226	2.807			
	4	3	1.521	1.933			
	5	3	1.026	1.292			
10	5	4	0.976	1.130	1.150		
	5	4	0.768	0.859	1.209		
	5	5	0.755	0.913	0.982	1.449	
15	6	5	0.491	0.519	0.781	1.006	
	7	5	0.334	0.420	0.430	0.668	
	8	5	0.176	0.242	0.380	0.353	
20	9	5	0.121	0.119	0.195	0.246	
	10	5	0.081	0.102	0.129	0.163	
	10	6	0.077	0.097	0.123	0.131	0.195
30	11	6	0.041	0.055	0.093	0.082	0.103
	12	6	0.027	0.152	0.044	0.055	0.070
30	12	6	0.016	0.011	0.026	0.037	0.122

modulus of fracture and Poisson's ratio caused by the roughness of the fracture. According to the data (Chang *et al.* 2004), the seepage coefficient of fractured rock mass under three dimensional conditions can be obtained

$$k = k_0 e^{-2[b(\sigma_2 - ap) - c(\sigma_1 + \sigma_3)]} \quad (9)$$

where k_0 is the initial permeability coefficient of fractured rock mass, a is the influence coefficient that takes into account the effect of fracture roughness on pore water pressure, b is the influence coefficient of roughness of

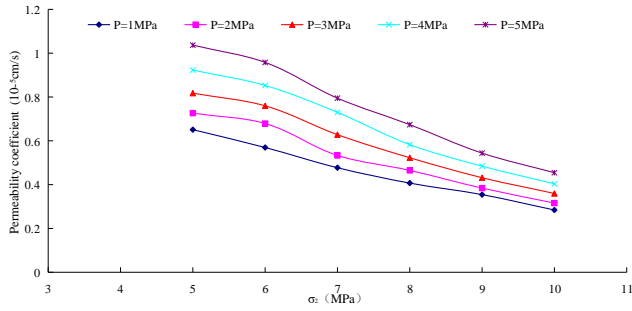


Fig. 12 Change rule of permeability coefficient with σ_2 increasing under different osmotic pressure

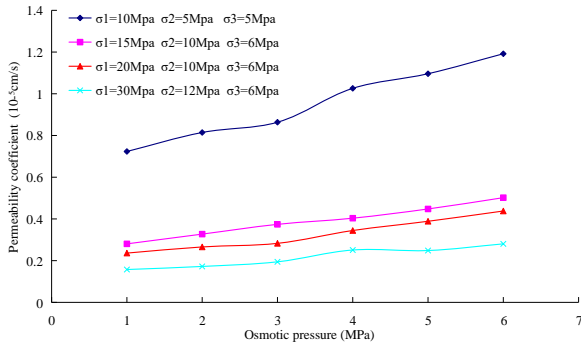


Fig. 13 Change rule of permeability coefficient with the osmotic pressure increasing under different stress conditions

fractures on the normal modulus of elasticity of a fracture, c is the coefficient of influence of the roughness of the fracture on the ratio of Poisson's ratio and tangential elastic modulus of the fracture.

Considering the roughness of specimen and formula (9), and then fitting the test results of permeability coefficient of #1 specimen, it can be expressed as

$$k = k_0 e^{-2[b(\sigma_2 - P) - c(\sigma_1 + \sigma_3)]}$$

$$= 0.000017 e^{-2[0.09365(\sigma_2 - 0.627P) + 0.00358(\sigma_1 + \sigma_3)]}$$
(10)

Fitting the test results of permeability coefficient of #2 specimen, it can be expressed as

$$k = k_0 e^{-2[b(\sigma_2 - P) - c(\sigma_1 + \sigma_3)]}$$

$$= 0.000084 e^{-2[0.1936(\sigma_2 - 0.597P) + 0.02485(\sigma_1 + \sigma_3)]}$$
(11)

The seepage coefficient changes rule under different osmotic pressures and stresses can be obtained, as shown in Figs. 12 and 13.

From the experimental results and the above analysis, it is found that σ_1 , σ_2 and σ_3 can inhibit the penetration of a single fissure, and the permeability coefficient decreases with the increase of σ_1 , σ_2 and σ_3 ; The influence of σ_2 on permeability is very evident and plays a leading role, the permeability coefficient decreases rapidly with the increase of σ_2 , and the permeability coefficient decreases obviously when σ_2 is greater than 6 MPa; According to Fig. 13, when the osmotic pressure is greater than 3 MPa, the permeability increases more obviously, which is more prominent when the three-dimensional stress is small.

Based on this analysis, owing to the deep mining coal seam floor rock is in a high stress state, but after mining, the load of the floor rock in goaf is changed, and the rock mass is changed from high stress to unloading state. Research shows that unloading fracture of rock mass under three axis high stress condition reduces the mechanical properties of rock, and the characteristics of tensile fracture are more prominent, and all kinds of fractured networks develop while the rock roughness on the fractured surface is evidently enhanced (Samanta *et al.* 2018, Alalaimi *et al.* 2015). Then, after the coal seam is mined, although the confined water pressure on the goaf floor does not change, the seepage characteristics of rock will be significantly enhanced due to the unloading effect, which is conducive to the formation and evolution of water inrush channels, the damage degree of water inrush also increased further, and this change is more pronounced with the increase of the mining depth. At the same time, the water inrush channels in the floor are more likely to evolve when the water pressure is higher than 3 MPa.

4. Conclusions

In this study, the permeability coefficient formula of single fracture surfaces was theoretically deduced under the condition of stress-seepage coupling; Large-scale fractured rock specimens were adopted in the seepage test, under different osmotic pressures and three-dimensional stresses to get the permeability coefficient, and the fitting formula of the permeability coefficient of the fractured rock was obtained.

For the fractured rock, the joint roughness, three-dimensional stress and water pressure all affect the seepage characteristics of the channel, and the water pressure has a positive correlation with permeability coefficient change; Under the certain water pressure, the permeability coefficient decreases when the three-dimensional stress increases; the influence of normal principal stress on permeability is obvious and plays a leading role.

Through the stress-seepage coupling test, the change of fractured seepage flow in mining floor and the favorable conditions for the water inrush channel evolution were analyzed, which provides theoretical guidance and reference for preventing water inrush from floor and similar research.

Acknowledgments

This research was financially supported by the National Natural Science Foundation of China (51974172), China Postdoctoral Science Foundation (2015M572067), Postdoctoral Innovation Project of Shandong Province (152799), Qingdao Postdoctoral Applied Research Project (2015203), Young Teachers' Growth Program of Shandong Province, Natural Science Foundation of Shandong Province (ZR2019MEE004) and the Shandong University of Science and Technology (SDUST) Research Fund (2018TDJH102).

References

Al-Shukur, A.H., Al-Qaisi, A.Z. and Al-Rammahi, A.M. (2018),

- “Nonlinear analysis of water-soil-barrage floor interaction”, *MATEC Web Conf.*, **162**.
- Alalaimi, M., Lorente, S., Wechsato, W. and Bejan, A. (2015), “The robustness of the permeability of constructal tree-shaped fissures”, *Int. J. Heat Mass Transfer*, **90**, 259-265. <https://doi.org/10.1016/j.ijheatmasstransfer.2015.06.042>.
- Bandis, S.C., Lumsden, A.C. and Barton, N.R. (1983), “Fundamentals of rock joint deformation”, *Int. J. Rock Mech. Min. Sci. Geomech. Abstr.*, **20**(6), 249-268. [https://doi.org/10.1016/0148-9062\(83\)90595-8](https://doi.org/10.1016/0148-9062(83)90595-8).
- Cai, M.F. He, M.C. and Liu, D.Y. (2002), *Rock Mechanics and Engineering*, Science Press, Beijing, China.
- Chang, Z.X., Zhao, Y.S., Hu, Y.Q. and Yang, D. (2004), “Theoretic and experimental studies on seepage law of single fracture under 3D stresses”, *Chin. J. Rock Mech. Eng.*, **23**(4), 620-624.
- Conrad, J. E., Prouty, N. G., Walton, M. A., Kluesner, J. W., Maier, K. L., McGann, M., Brothers, D.S., Roland, E.C. and Dartnell, P. (2018), “Seafloor fluid seeps on Kimki Ridge, offshore southern California: Links to active strike-slip faulting”, *Deep-Sea Res. Part II Top. Stud. Oceanogr.*, **150**, 82-91. <https://doi.org/10.1016/j.dsr2.2017.11.001>.
- Develi, K. and Babadagli, T. (2015), “Experimental and visual analysis of single-phase flow through rough fracture replicas”, *Int. J. Rock Mech. Min. Sci.*, **73**, 139-155. <https://doi.org/10.1016/j.ijrmms.2014.11.002>.
- Di, S.T., Jia, C., Qiao, W.G., Yu, W.J. and Li, K. (2017), “Theoretical and experimental investigation of characteristics of single fracture stress-seepage coupling considering microroughness”, *J. Math Probl. Eng.*, **12**, 1-12. <https://doi.org/10.1155/2017/6431690>.
- Giwelli, A.A., Matsuki, K., Sakaguchi, K. and Kizaki, A. (2014), “Effects of non-uniform traction and specimen height in the direct shear test on stress and deformation in a rock fracture”, *Int. J. Numer. Anal. Meth. Geomech.*, **37**(14), 2186-2204. <https://doi.org/10.1002/nag.2129>.
- Goodman, R.E. (1976), *Methods of Geological Engineering in Discontinuous Rocks*, West Publishing Company, New York, U.S.A.
- Haeri, H., Shahriar, K., Marji, M.F. and Mohammad, P. (2014), “Cracks coalescence mechanism and cracks propagation paths in rock-like specimens containing pre-existing random cracks under compression”, *J. Central South Univ.*, **21**(6), 2404-2414. <https://doi.org/10.1007/s11771-014-2194-y>.
- Jaksa, M.B. (2007), “Seepage properties of a single rock fracture subjected to triaxial stresses”, *J. Prog. Nat. Sci.*, **17**(12), 1482-1485.
- Javadi, M., Sharifzadeh, M. and Shahriar, K. (2010), “A new geometrical model for non-linear fluid flow through rough fractures”, *J. Hydrol.* **389**(1-2), 18-30. <http://doi.org/10.1016/j.jhydrol.2010.05.010>.
- Kong, D.Z., Cheng, Z.B. and Zheng, S.S. (2019), “Study on failure mechanism and stability control measures in large-cutting-height coal mining face with deep-buried seam”, *Bull. Eng. Geol. Environ.*, 1-15. <https://doi.org/10.1007/s10064-019-01523-0>.
- Konsoer, K.M., Rhoads, B.L., Langendoen, E.J., Best, J.L. and Garcia, M.H. (2015), “Spatial variability in bank resistance to erosion on a large meandering, mixed bedrock-alluvial river”, *Geomorphology*, **252**, 80-97. <https://doi.org/10.1016/j.geomorph.2015.08.002>.
- Lei, J.S. Li, S., Wu, Z.L., Yao, Q. and Zeng, Y.W. (2016), “Experimental study of shear displacement effect seepage characteristics of random surface cracks”, *Chin. J. Rock Mech. Eng.*, **35**(2), 3898-3899.
- Li, L.P., Chen, D.Y., Li, S.C., Shi, S.S., Zhang, M.G. and Liu, H.L. (2017), “Numerical analysis and fluid-solid coupling model test of filling-type fracture water inrush and mud gush”, *Geomech. Eng.*, **13**(6), 1011-1025. <https://doi.org/10.12989/gae.2017.13.6.1011>.
- Liolios, P.A. and Exadaktylos, G.E. (2006), “A solution of steady-state fluid flow in multiply fractured isotropic porous media”, *Int. J. Solids Struct.*, **43**(13), 3960-3982. <https://doi.org/10.1016/j.ijsolstr.2005.03.021>.
- Liu, C.H. and Chen, C.X. (2007), “The seepage characteristics of single fractured rock under triaxial stress”, *J. Prog. Nat. Sci.*, **17**(7), 989-994.
- Liu, T., Cao, P. and Lin, H. (2013), “Evolution procedure of multiple rock cracks under seepage pressure”, *Math Probl. Eng.*, 1-11. <https://doi.org/10.1155/2013/738013>.
- Louis, C. (1987), *Rock Hydraulics*, Springer-Verlag, New York, U.S.A.
- Lv, H.Y., Tang, Y.S., Zhang, L.F., Cheng, Z.B. and Zhang, Y.N. (2019), “Analysis for mechanical characteristics and failure models of coal specimens with non-penetrating single crack”, *Geomech. Eng.*, **17**(4), 355-365. <https://doi.org/10.12989/gae.2019.17.4.355>.
- Miao, T.J., Yu, B.M., Duan, Y.G. and Fang, Q.T. (2015), “A fractal analysis of permeability for fractured rocks”, *Int. J. Heat Mass Transfer*, **81**, 75-80. <http://doi.org/10.1016/j.ijheatmasstransfer.2014.10.010>.
- Morrow, C.A., Zhang, B.C. and Byerlee, J.D. (1986), “Effective pressure law for permeability of Westerly granite under cyclic loading”, *J. Geophys. Res.*, **91**(B3), 3870-3876. <https://doi.org/10.1029/JB091iB03p03870>.
- Nguyen-Thoi, T., Phung-Van, P., Ho-Huu, V. and Le-Anh, L. (2015), “An edge-based smoothed finite element method (ES-FEM) for dynamic analysis of 2D Fluid-Solid interaction problems”, *KSCE J. Civ. Eng.*, **19**(3), 641-650. <https://doi.org/10.1007/s12205-015-0293-4>.
- Odintsev, V.N. and Miletchenko, N.A. (2015) “Water inrush in mines as a consequence of spontaneous hydrofracture”, *J. Min. Sci.*, **51**(3), 423-434. <https://doi.org/10.1134/S1062739115030011>.
- Pham, K., Kim, D., Choi, H.J., Lee, I.M. and Choi, H. (2018), “A numerical framework for infinite slope stability analysis under transient unsaturated seepage conditions”, *Eng. Geol.*, **243**, 36-49. <http://doi.org/10.1016/j.enggeo.2018.05.021>.
- Samanta, M., Punetha, P. and Sharma, M. (2018), “Effect of roughness on interface shear behavior of sand with steel and concrete surface”, *Geomech. Eng.*, **14**(4), 387-398. <https://doi.org/10.12989/gae.2018.14.4.387>.
- Shao, J.L., Zhou, F. and Sun, W.B. (2019), “Evolution model of seepage characteristics in the process of water inrush in faults”, *Geofluids*, 1-14. <https://doi.org/10.1155/2019/4926768>.
- Snow, D.T. (1968), “Rock fracture spacings, openings, and porosities”, *J. Soil Mech.*, **94**(SM1), 73-91.
- Sun, W.B. and Xue, Y.C. (2018), “An improved fuzzy comprehensive evaluation system and application for risk assessment of floor water inrush in deep mining”, *Geotech. Geol. Eng.*, **37**(3), 1135. <https://doi.org/10.1007/s10706-018-0673-x>.
- Sun, W.B., Du, H.Q., Zhou, F. and Shao, J.L. (2019), “Experimental study of crack propagation of rock-like specimens containing conjugate fractures”, *Geomech. Eng.*, **17**(4), 323-331. <https://doi.org/10.12989/gae.2019.17.4.323>.
- Sun, W.B., Xue, Y.C., Li, T.T. and Liu, W.T. (2019), “Multi-field coupling of water inrush channel formation in a deep mine with a buried fault”, *Mine Water Environ.*, <https://doi.org/10.1007/s10230-019-00616-2>.
- Tao Y. and Liu, W.Q. (2012), “An equivalent seepage resistance model with seepage-stress coupling for fractured rock mass”, *Rock Soil Mech.*, **33**(7), 2041-2042.
- Tsang Y.W. and Tsang, C.F. (2004), “Channel model of flow through fractured media”, *Water Resour. Res.*, **23**(3), 467-479. <https://doi.org/10.1029/WR023i003p00467>.

- Tse, R. and Cruden, D.M. (1979), "Estimating joint roughness coefficients", *Int. J. Rock Mech. Min. Sci. Geomech. Abstr.*, **165**(5), 303-307. [https://doi.org/10.1016/0148-9062\(79\)90241-9](https://doi.org/10.1016/0148-9062(79)90241-9).
- Wu, Y.X. (2010), "Modelling rough joint network and study on hydro-mechanical Behavior of Fractured Rock Mass", Ph.D. Dissertation, Institute of Rock and Soil Mechanics, Chinese Academy of Sciences, Wuhan, China.
- Xu, C.W., Nie, W., Liu, Z.Q., Peng, H.T., Yang, S.B. and Liu, Q. (2019), "Multi-factor numerical simulation study on spray dust suppression device in coal mining process", *Energy*, **182**, 544-558. <https://doi.org/10.1016/j.energy.2019.05.201>.
- Yang, T.H., Jia, P., Shi, W.H., Wang, P.T., Liu, H.L. and Yu, Q.L. (2014), "Seepage-stress coupled analysis on anisotropic characteristics of the fractured rock mass around roadway", *Tunn. Undergr. Sp. Technol.*, **43**, 11-19. <https://doi.org/10.1016/j.tust.2014.03.005>.
- Yasuhara, H., Polak, A., Mitani, Y., Grader, A.S., Halleck, P.M. and Elsworth, D. (2006), "Evolution of fracture permeability through fluid-rock reaction under hydrothermal conditions", *Earth Plan. Sci. Lett.*, **244**(1-2), 186-200. <https://doi.org/10.1016/j.epsl.2006.01.046>.
- Yu, H.D., Chen, F.F., Chen, W.Z., Yang, J.P., Cao, J.J. and Yuan, K.K. (2012) "Research on permeability of fractured rock", *Chin. J. Rock Mech. Eng.*, **31**(1), 2788-2795.
- Zhang, Y.Z. and Zhang, J.C. (1997), "Experimental study of the seepage flow-stress coupling in fractured rock masses", *Rock Soil Mech.*, **18**(4), 59-62.